

1 **Turbulence Generation in High-power Laser-Plasma Interaction Relevant** 2 **to Astrophysical Scenarios**

3 Indraj Singh*, R. Uma, and R. P. Sharma

4 *Department of Energy Science and Engineering, Indian Institute of Technology Delhi, India*

5

6 **Abstract**

7 Many astrophysical scenarios such as supernova remnant (SNR), Cassiopeia A, the collision
8 of galaxies, turbulent magnetic field amplification in the intergalactic medium, etc., have
9 been imitated by utilizing high-power lasers. A hundred times stronger magnetic field has
10 been observed in Cassiopeia A than in the adjacent interstellar medium. It is presumed that
11 the surrounding clumpy media near supernova remnant Cassiopeia A support myriads modes,
12 which act as a source for amplifying the turbulent magnetic field. The origin of magnetic
13 field amplification in the clumpy medium is not fully understood yet. The typical model for
14 this amplification is the seed field amplification due to turbulence generation. Such magnetic
15 field amplification and turbulence generation have been reported experimentally in laboratory
16 astrophysics. A model is proposed to study the turbulence generation and magnetic field
17 amplification, which ensues due to the high-power laser interaction with plasma. In this
18 study, we employed computational techniques to solve the coupled system of the model
19 equations.

20 **Email*:** indraj436@gmail.com

21

22 **Introduction**

23 In laboratory astrophysics, the amplification of the magnetic field has been observed in the
24 laboratory experiments relevant to the many astrophysical phenomena like supernova
25 remnant (SNR), Cassiopeia A, the collision of galaxies, etc. [1-4]. The present investigation
26 is motivated by the laboratory experiments in which up to megagauss order amplification of
27 the magnetic field is observed [1]. A nonlinear wave-wave coupling model is developed
28 between the x-mode laser and the upper hybrid wave. The relativistic electron mass variation
29 and nonlinear ponderomotive force are considered in this model.

30 **Model equations for the dynamics:**

31 The expressions for the electric field for the x-mode laser and upper hybrid wave are given by

$$32 \quad \vec{E}_l = |E_{lx}\hat{x} + E_{ly}\hat{y}| \exp\{-i(\omega_l t - k_l x)\} \quad (1)$$

$$33 \quad \vec{E}_u = \hat{x}E_{ux} \exp\{-i(\omega_u t - k_u x)\} \quad (2)$$

34 Where, $k_l(k_u)$ and $\omega_l(\omega_u)$ are symbolize the propagation constant and the angular frequency
 35 of pump wave (upper hybrid wave), respectively. Now, the wave equation governing the
 36 dynamics can be written as

$$37 \quad \nabla^2 \vec{E} - \nabla(\nabla \cdot \vec{E}) = \frac{4\pi}{c^2} \frac{\partial J}{\partial t} + \frac{1}{c^2} \frac{\partial^2 E}{\partial t^2} \quad (3)$$

38 The nonlinear coupled dynamical equations for the x-mode laser and upper hybrid wave have
 39 been developed. The coupled dynamical equations in the normalized form can be written as

$$40 \quad i \frac{\partial E_{ly}}{\partial t} + iC_1 \frac{\partial E_{ly}}{\partial x} + \frac{\partial^2 E_{ly}}{\partial x^2} + \frac{\partial^2 E_{ly}}{\partial z^2} = nE_{ly} - C_2 |E_{ly}|^2 E_{ly} = 0 \quad (4)$$

$$41 \quad \frac{\partial^2 n}{\partial t^2} + C_3 \frac{\partial^2 n}{\partial x^2} + n = \frac{\partial^2 |E_{ly}|^2}{\partial x^2} + C_4 \frac{\partial^2 |E_{ly}|^2}{\partial z^2} \quad (5)$$

42 Equation (4) is the dynamical equation for the x-mode laser, and equation (5) denotes the
 43 dynamical equation for the upper hybrid wave. The normalizing parameters and constants are

$$44 \quad t_n \approx \omega_l^{-1}, \quad x_n = z_n = \sqrt{\frac{c^2 t_n}{2\omega_l}}, \quad n_n = \frac{2\omega_l n_0 (\omega_l^2 - \omega_{ce}^2 - \omega_{pe}^2)}{\omega_{pe}^2 t_n (\omega_l^2 - \omega_{pe}^2)}, \quad E_n = \sqrt{\frac{16\pi m_e x_n^2 n_n (\omega_{ce}^2 + \omega_{pe}^2)}{\omega_{pe}^2 t_n^2}},$$

$$45 \quad C_1 = \sqrt{\frac{2k_l^2 c^2 t_n}{\omega_l}}, \quad C_2 = \frac{e^2 E_n^2 \omega_{pe}^2 t_n (\omega_l^2 - \omega_{pe}^2)}{4c^2 \omega_l^3 m_e^2 (\omega_l^2 - \omega_{ce}^2 - \omega_{pe}^2)}, \quad C_3 = \frac{t_n^2 v_{te}^2}{x_n^2}, \quad C_4 = \frac{x_n^2}{z_n^2},$$

46 Where v_{te} symbolize the electron thermal speed, ω_{ce} and ω_{pe} are the electron cyclotron
 47 frequency and electron plasma frequency, respectively.

48 **Results and Discussion:**

49 To solve the normalized equations (4) and (5) the following initial conditions are utilized

$$50 \quad \vec{E}_k(x, z, 0) = |E_0| \{1 + 0.1 \cos(\alpha_x x)\} \{1 + 0.1 \cos(\alpha_z z)\} \quad (6)$$

$$n(x, z) = -\sum_k |E_k(x, z)|^2 \quad (7)$$

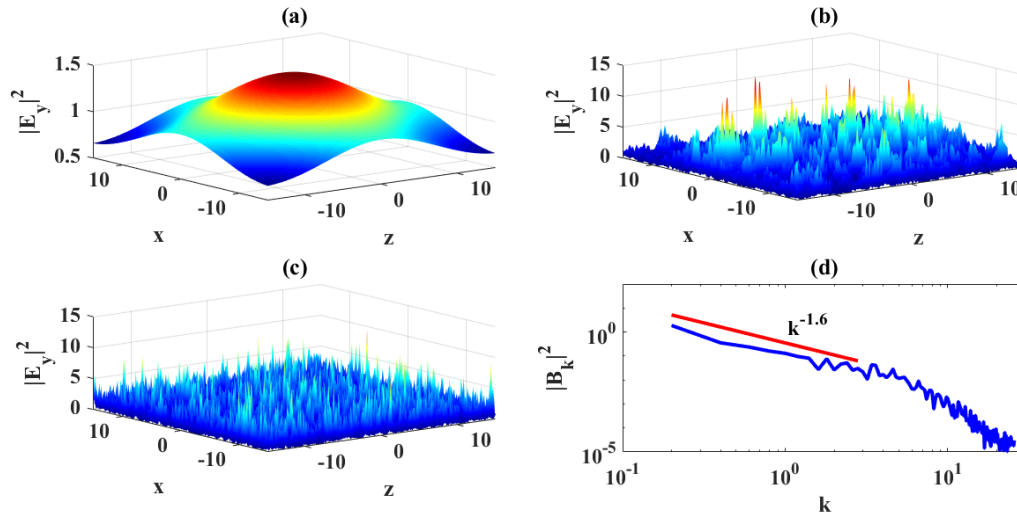
52 Where the initial amplitude $E_0 = 1$ and the perturbation wavenumbers $\alpha_x, \alpha_z = 0.2$. A periodic
 53 box with periodicity $2\pi / \alpha_x \times 2\pi / \alpha_z$, grid points 256×256 , and step size $\sim 10^{-5}$ are utilized
 54 for the computational simulation. For the computational simulation, the finite difference has
 55 been employed in time, the pseudo-spectral method is used in space, and all parameters have
 56 been taken (not exact parameters) according to the Mondal et al.¹ experiments. The numerical
 57 values of normalizing parameters used in computational simulations are $B_0 = 1 \text{ MG}$,
 58 $\omega_0 = 5.25 \times 10^{14} \text{ rad/sec}$, $n_0 = 9.75 \times 10^{17} \text{ cm}^{-3}$, $T_e = 3 \text{ eV}$, $n_n \approx 0.01 n_0$, $t_n \approx 2 \text{ psec}$, $x_n = z_n \approx 5 \mu\text{m}$. The
 59 accuracy of the algorithm has been verified with the well-known nonlinear Schrodinger
 60 equation and modified accordingly for this dynamics. The pump wave exerts a nonlinear
 61 ponderomotive force on the upper hybrid wave, resulting in a modification in the background
 62 density. When the pump wave propagates in the perturbed background density, the
 63 localization of the pump wave takes place, which becomes chaotic with time. The generation
 64 of the localized structures of the pump wave in the magnetic field plays an essential role in
 65 the turbulence generation in the self-generated magnetic field. From the simulation results,
 66 the magnetic field amplification up to 3-4 times has been observed, as shown in the figure.
 67 The figures also depict the time-averaged magnetic turbulence generation with power-law
 68 scaling ($k^{-1.6}$) observed from the simulation results.

69 **Conclusion:**

70 This investigation describes a nonlinear wave-wave coupling model in the magnetized
 71 plasma. The background magnetic field is considered along the perpendicular direction to
 72 both the electric field direction and the direction of the propagation constant. A nonlinear
 73 wave-wave coupling model is developed by taking into account the relativistic electron mass
 74 variation and nonlinear ponderomotive force and solved by computational simulations. The
 75 magnetic field amplification and the turbulence generation have been observed from the
 76 simulation results.

77

78 **Figures:**



79

80 **Figure:** The normalized field intensity in the z - x plane at the different normalized times (t)
 81 (a)0, (b)18, (c)30, and (d) the time-averaged magnetic turbulence between the normalized
 82 time 17-24 containing seven spectra.

83 **Acknowledgement:**

84 This research is supported by the Department of Science and Technology (DST), India.

85 **References:**

- 86 1. S. Mondal, V. Narayanan, Wen Jun Ding, Amit D. Lad, Biao Hao, Saima Ahmad, Wei Min Wang,
 87 Zheng Ming Sheng, Sudip Sengupta, Predhiman Kaw, Amita Das, and G. Ravindra Kumar, “Direct
 88 observation of turbulent magnetic fields in hot, dense laser produced plasmas,” Proc. Natl. Acad. Sci.,
 89 109, 8011-8015 (2012).
- 90 2. J. Meinecke, H. W. Doyle, F. Miniati, A. R. Bell, R. Bingham, R. Crowston, R. P. Drake, M.
 91 Fatenejad, M. Koenig, Y. Kuramitsu, C. C. Kuranz, D. Q. Lamb, D. Lee, M. J. MacDonald, C. D.
 92 Murphy, H.-S. Park, A. Pelka, A. Ravasio, Y. Sakawa, A. A. Schekochihin, A. Scopatz, P. Tzeferacos,
 93 W. C. Wan, N. C. Woolsey, R. Yurchak, B. Reville, and G. Gregori, “Turbulent amplification of
 94 magnetic fields in laboratory laser produced shock waves,” Nat. Phys. 10, 520–524 (2014).
- 95 3. J. Meinecke, P. Tzeferacos, A. Bella, R. Binghamc, R. Clarke, E. Churazove, R. Crowstong, H.
 96 Doylea, R. P. Drakeh, R. Heathcote, M. Koenigi, Y. Kuramitsu, C. Kuranz, D. Lee, M. MacDonald, C.
 97 Murphy, M. Notley, H. S. Park, A. Pelka, A. Ravasio, B. Reville, Y. Sakawa, W. Wan, N. Woolsey, R.
 98 Yurchak, F. Miniati, A. Schekochihin, D. Lamb, and G. Gregori, “Developed turbulence and nonlinear
 99 amplification of magnetic fields in laboratory and astrophysical plasmas,” Proc. Natl. Acad. Sci. 112,
 100 8211-8215 (2015).
- 101 4. P. Tzeferacos, A. Rigby, A. F. A. Bott, A. R. Bell, R. Bingham, A. Casner, F. Cattaneo, E. M.
 102 Churazov, J. Emig, F. Fiuza, C. B. Forest, J. Foster, C. Graziani, J. Katz, M. Koenig, C.-K. Li, J.
 103 Meinecke, R. Petrasso, H.-S. Park, B. A. Remington, J. S. Ross, D. Ryu, D. Ryutov, T. G. White, B.
 104 Reville, F. Miniati, A. A. Schekochihin, D. Q. Lamb, D. H. Froula, and G. Gregori, “Laboratory
 105 evidence of dynamo amplification of magnetic fields in a turbulent plasma,” Nat. Commun. 9, 591
 106 (2018).